

Supporting Information

Highly Reversible and Stable Zn Metal Anodes Realized by Trifluoroacetamide Electrolyte Additive

Miaomiao Wu, Xingchao Wang,* Fei Zhang, Qian Xiang, Yan Li and Jixi Guo*

State Key Laboratory of Chemistry and Utilization of Carbon Based Energy Resources; Key Laboratory of Advanced Functional Materials, Autonomous Region; Institute of Applied Chemistry, College of Chemistry, Xinjiang University, Urumqi, 830046, Xinjiang, P. R. China.

Email: ichemabc@126.com, jxguo1012@163.com

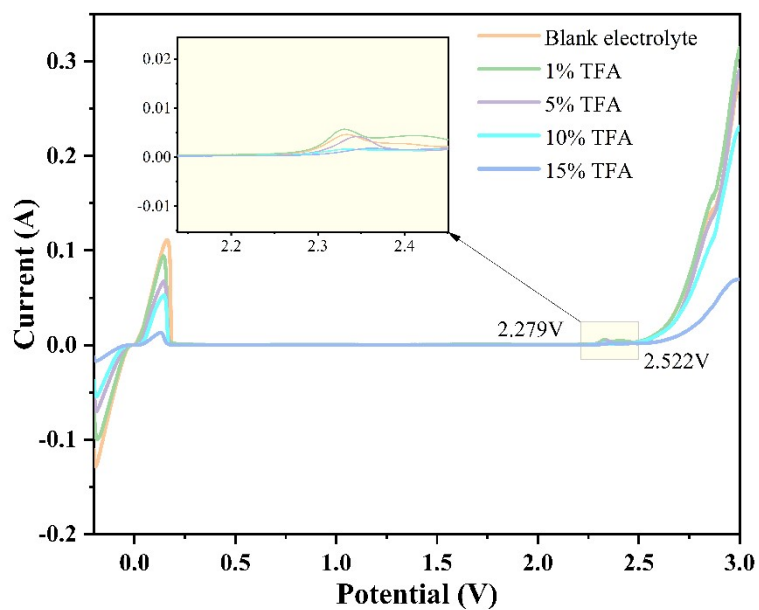


Figure S1 LSV of Zn//SS cells containing blank electrolyte and electrolytes with different TFA content.

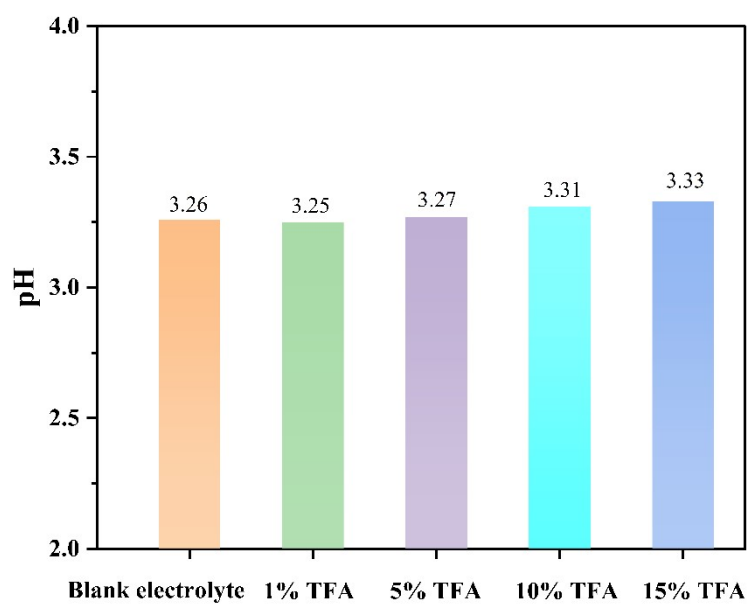


Figure S2 pH values of blank electrolyte and electrolytes with different TFA content.

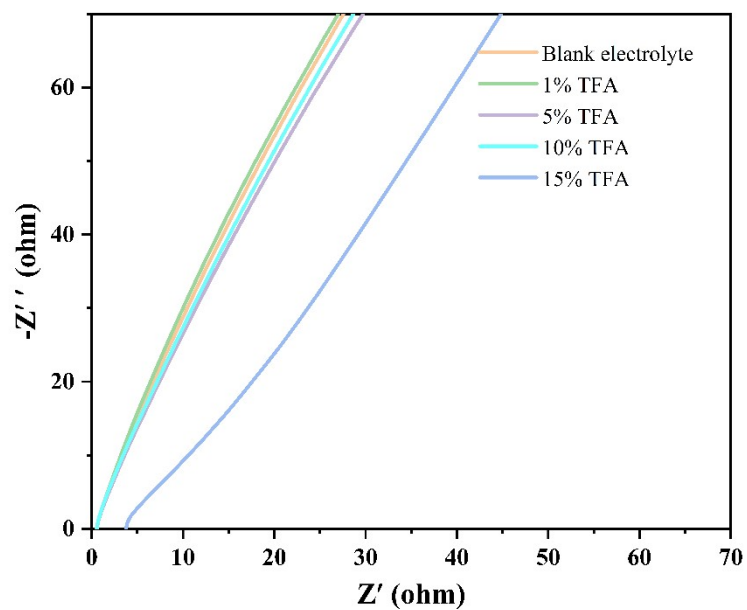


Figure S3 EIS curves of SS//SS cells with blank electrolyte and electrolytes with different TFA content.

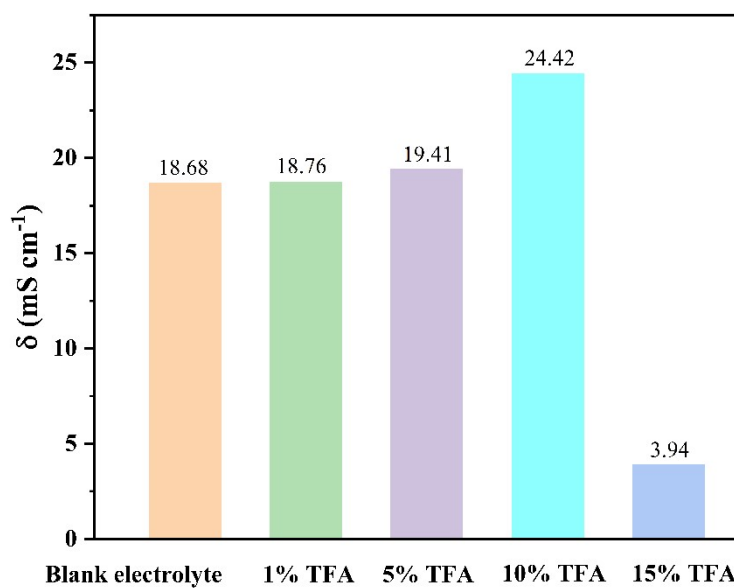


Figure S4 Ionic conductivities of blank electrolyte and electrolytes with different TFA content.

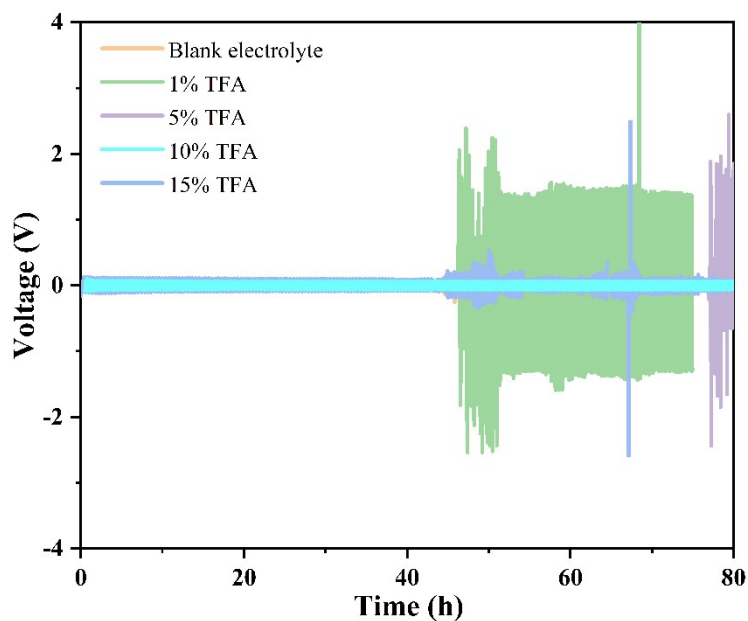


Figure S5 Time-voltage profiles of Zn//Zn cells containing blank electrolyte and electrolytes with different TFA content at 5 mA cm^{-2} and 1 mAh cm^{-2} .

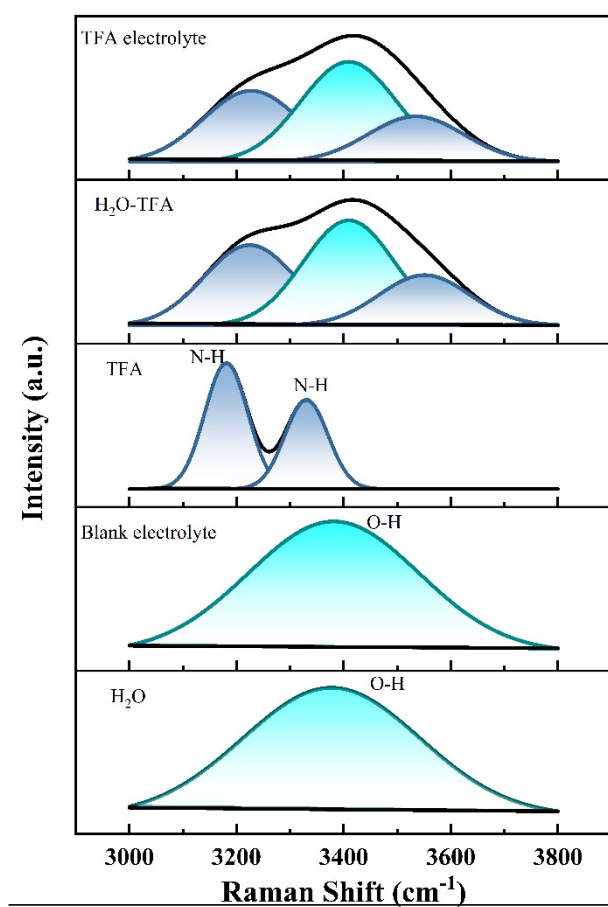


Figure S6 Raman spectra of H_2O solvent, blank and TFA electrolytes, H_2O -TFA (10% TFA) mixture, and TFA, respectively.

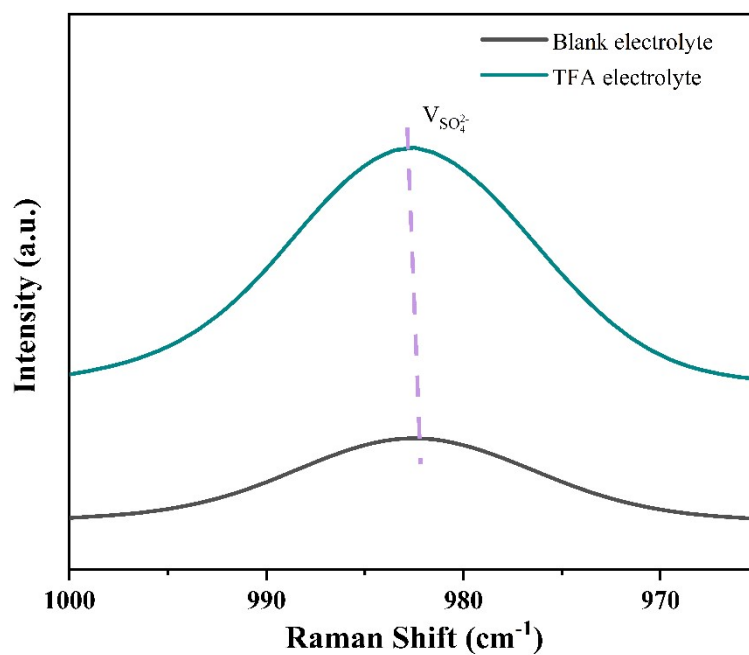


Figure S7 Raman spectra of blank and TFA electrolytes within the range of 965-1000 cm^{-1} .

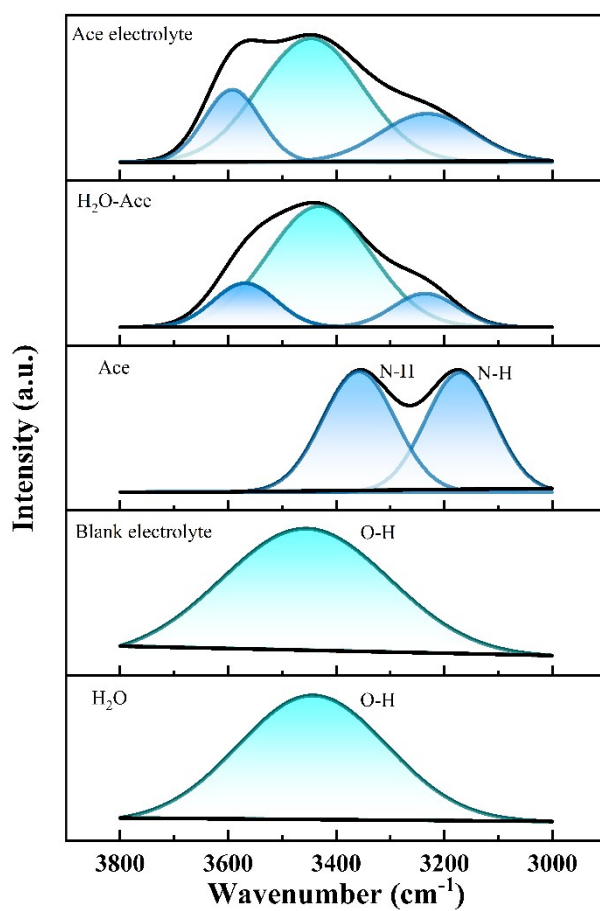


Figure S8 FTIR spectra of H_2O solvent, blank electrolyte, Ace, H_2O -Ace (10% Ace) mixture, and Ace (10% Ace) electrolyte, respectively.

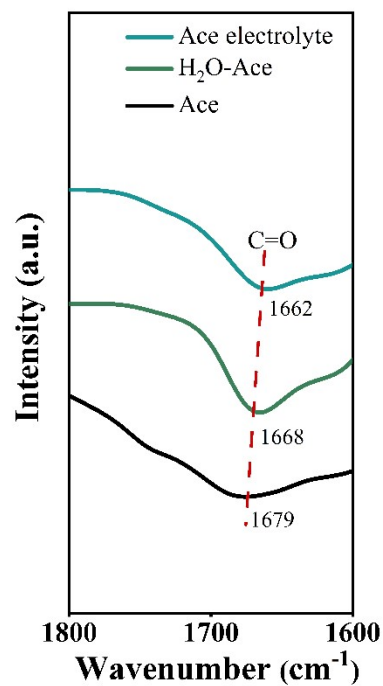


Figure S9 FTIR spectra of Ace, H₂O-Ace (10% Ace) mixture and Ace (10% Ace) electrolyte within the range of 1600-1800 cm⁻¹.

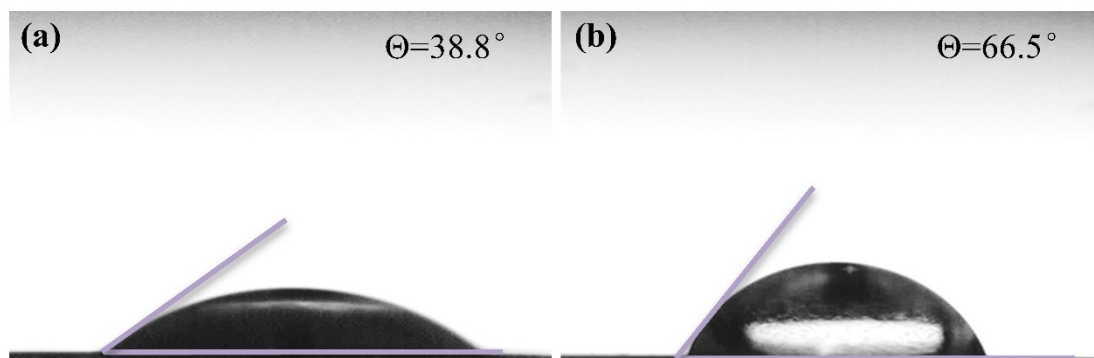


Figure S10 The contact angle of (a) TFA and (b) blank electrolytes on Zn foil.

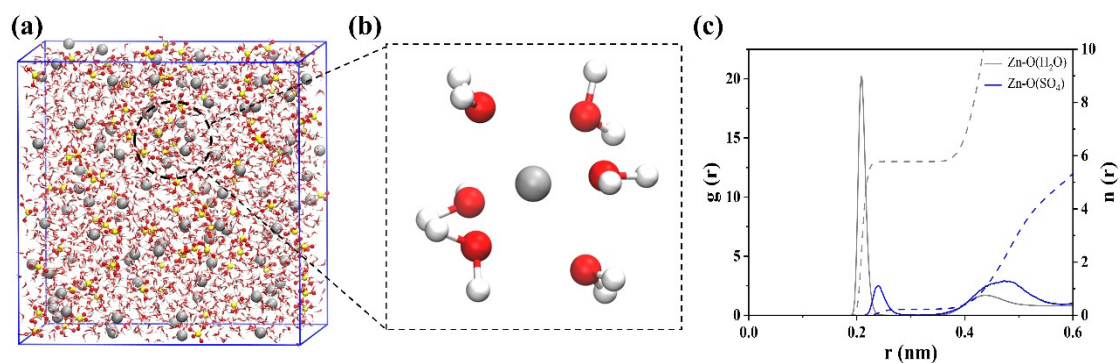


Figure S11 (a) 3D snapshot of blank electrolyte from MD simulation and (b) partial enlarged snapshot representing the electrolyte structure. (c) The radial distribution function (RDF) $g(r)$ and corresponding integrated coordination numbers $n(r)$ of Zn^{2+} -O (for H_2O) and Zn^{2+} -O (for SO_4^{2-}).

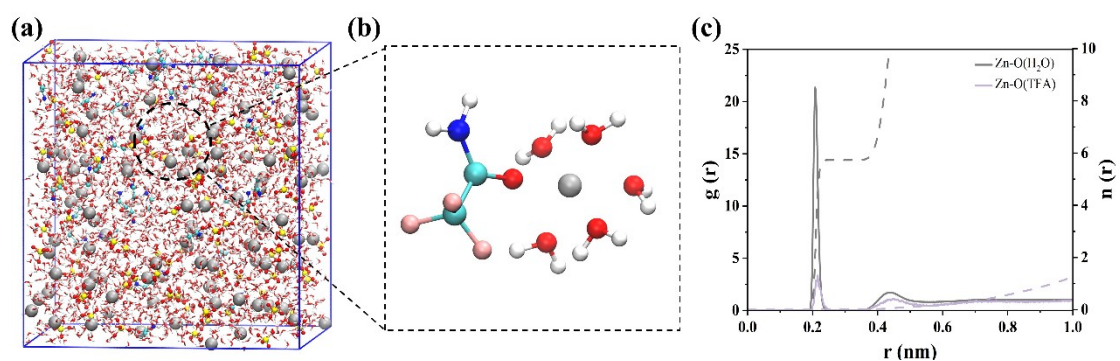


Figure S12 (a) 3D snapshot of 5%TFA electrolyte from MD simulation and (b) partial enlarged snapshot representing the electrolyte structure. (c) The radial distribution function (RDF) $g(r)$ and corresponding integrated coordination numbers $n(r)$ of Zn^{2+} -O (for H_2O) and Zn^{2+} -O (for TFA).

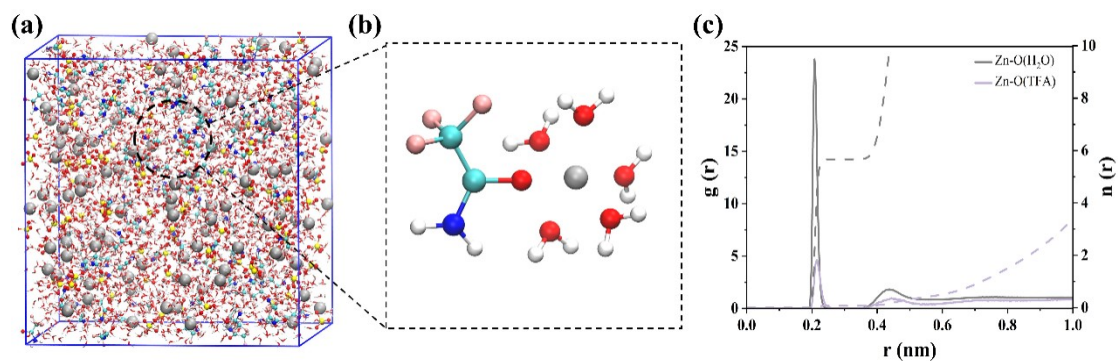


Figure S13 (a) 3D snapshot of 15%TFA electrolyte from MD simulation and (b) partial enlarged snapshot representing the electrolyte structure. (c) The radial distribution function (RDF) $g(r)$ and corresponding integrated coordination numbers $n(r)$ of Zn^{2+} -O (for H_2O) and Zn^{2+} -O (for TFA).

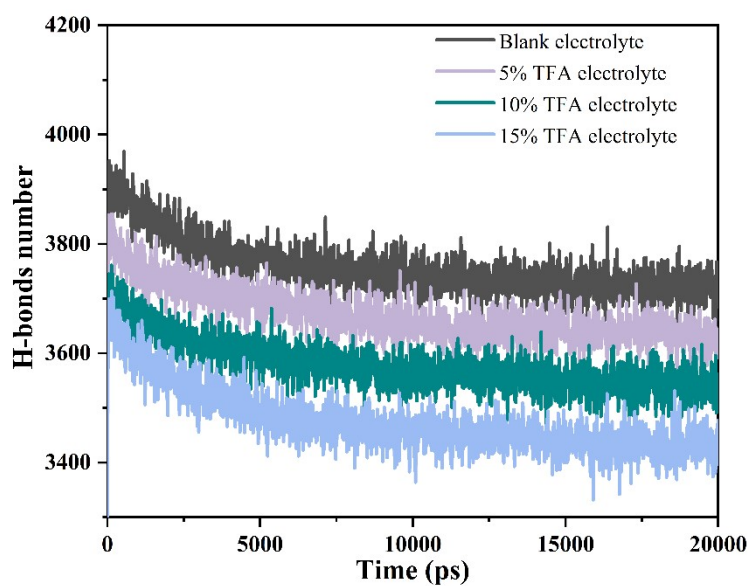


Figure S14 Number counts for hydrogen bonds of H_2O molecules for blank electrolyte and electrolytes with different TFA content.

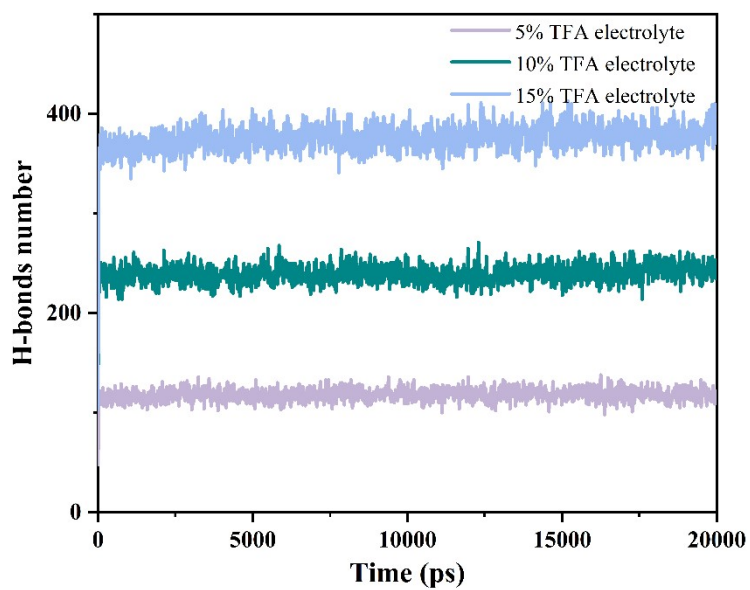


Figure S15 Number counts for hydrogen bonds of H₂O and TFA in electrolytes with different TFA content.

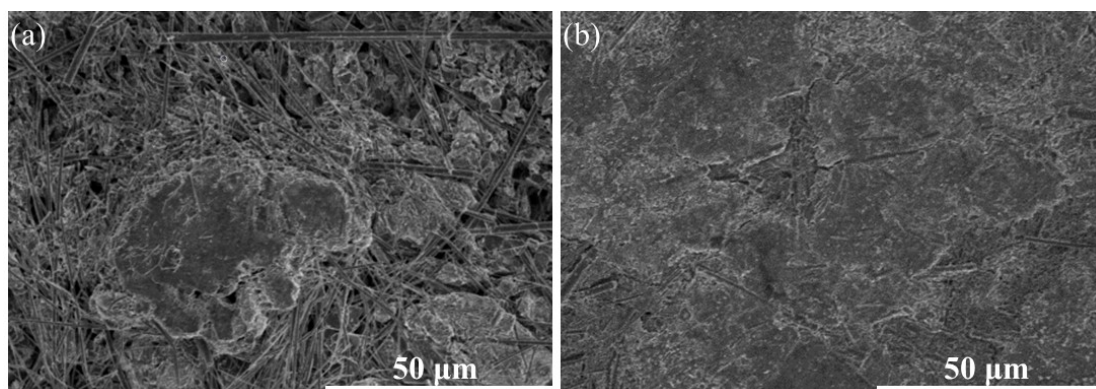


Figure S16 SEM images of the Zn anodes morphology after cycling for 100 h at 5 mA cm⁻² in (a) blank and (b) TFA electrolytes.

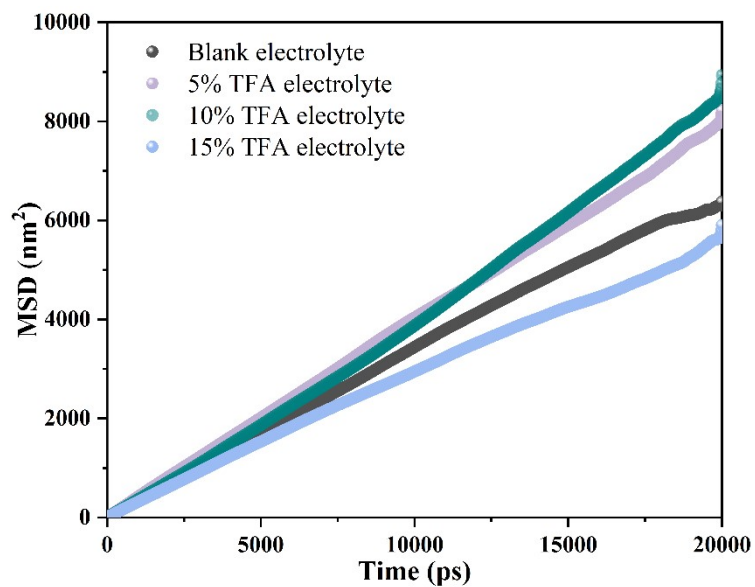


Figure S17 The function of MSD vs. time in blank electrolyte and electrolytes with different TFA content.

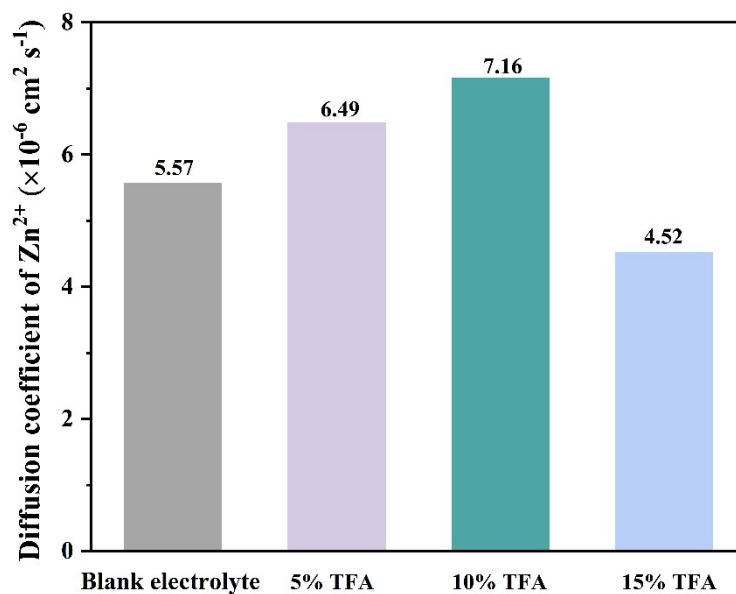


Figure S18 The diffusion coefficient of Zn²⁺ in blank electrolyte and electrolytes with different TFA content.

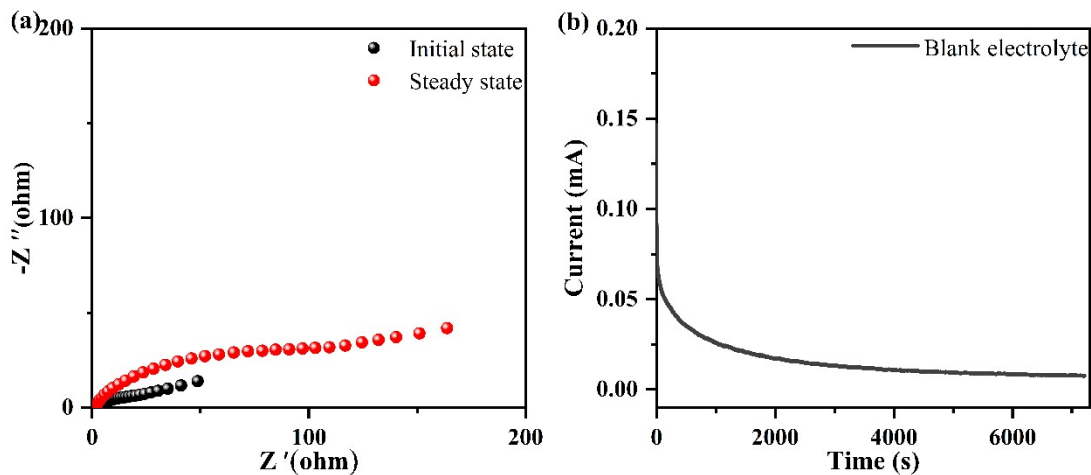


Figure S19 (a) Nyquist plots of Zn//Zn symmetric cells in blank electrolyte before/after potentiostatic polarization. (b) Current variations of Zn//Zn symmetric cells at room temperature with potentiostatic polarization at 10 mV in blank electrolyte.

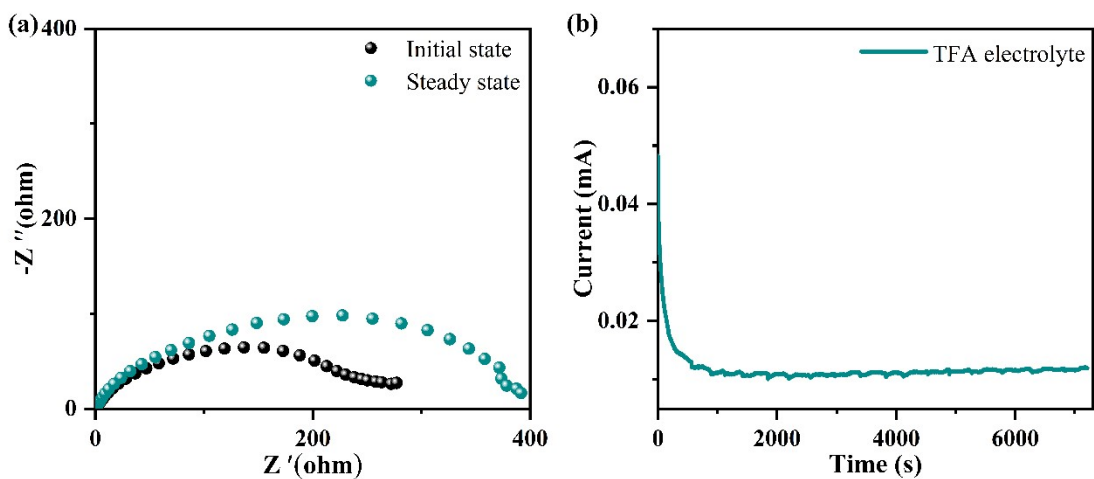


Figure S20 (a) Nyquist plots of Zn//Zn symmetric cells in TFA electrolyte before/after potentiostatic polarization. (b) Current variations of Zn//Zn symmetric cells at room temperature with potentiostatic polarization at 10 mV in TFA electrolyte.

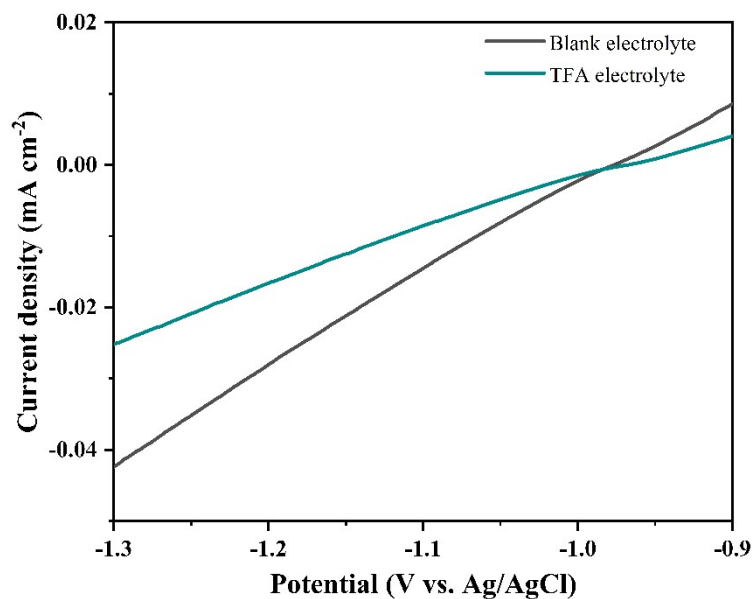


Figure S21 Hydrogen evolution polarization curves of blank and TFA electrolytes.

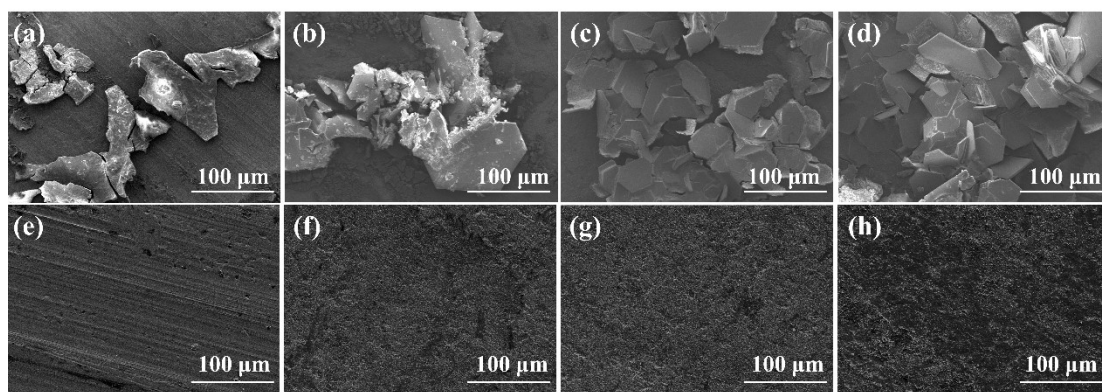


Figure S22 SEM images of Zn foils soaked in (a-d) blank and (e-f) TFA electrolytes after (a, e) 1 day, (b, f) 5 days, (c, g) 10 days and (d, h) 15 days, respectively.

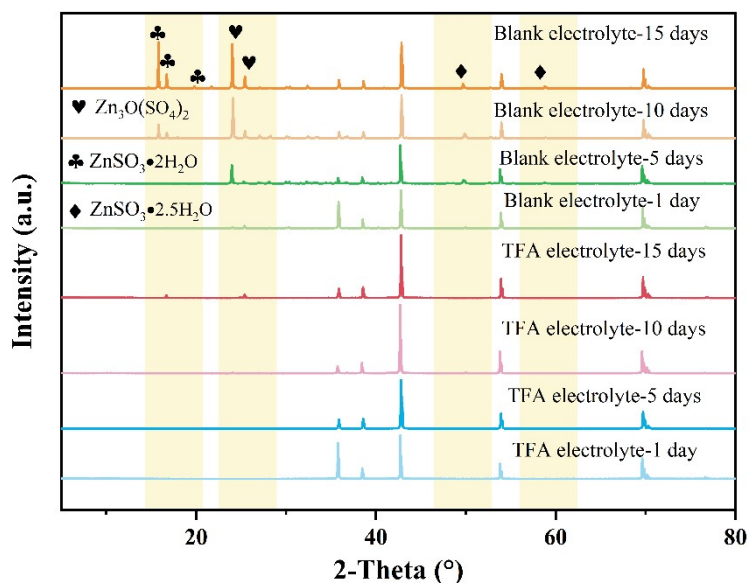


Figure S23 XRD patterns of Zn foils soaked in blank and TFA electrolytes after different days.

The morphologies of Zn anodes in blank and TFA electrolytes were investigated using SEM after different immersion times. As shown in Figures S20a-d, in the blank electrolyte, severe irregular protruding structures appeared on the Zn anode surface with increasing immersion time. In contrast, in TFA electrolyte, even after 15 days of immersion, no obvious by-products were observed on the Zn anode surface, suggesting that TFA inhibits the corrosion of the Zn anode (Figure S20e-h). The physical phases of the by-products generated during the immersion of the Zn anode in different electrolytes were also investigated. After immersing the Zn anode in TFA electrolyte for up to 15 days, only a weak characteristic peak of by-products was observed (Figure S21). On the other hand, even after just 1 day of immersion in the blank electrolyte, the Zn anode showed weak characteristic peaks of by-products. Furthermore, after extending the immersion period to 15 days, the diffraction characteristic peaks of the by-products $\text{Zn}_3\text{O}(\text{SO}_4)_2$, $\text{ZnSO}_3 \cdot \text{H}_2\text{O}$ and $\text{ZnSO}_3 \cdot 2\text{H}_2\text{O}$ became very obvious. These results further demonstrate the inhibition effect of TFA on corrosion and side reactions of Zn anode.

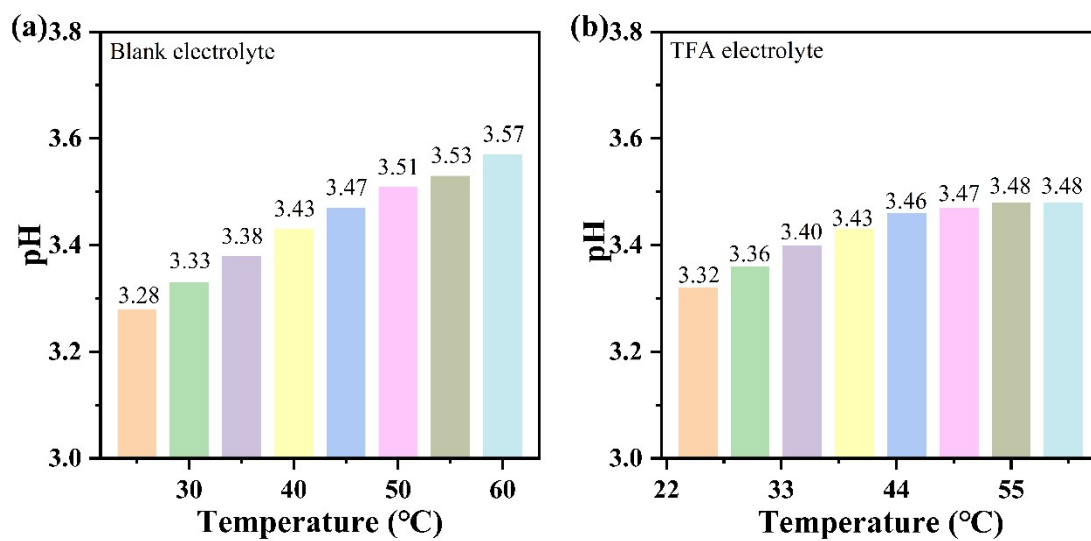


Figure S24 pH value of (a) blank electrolyte and (b) TFA electrolyte at different temperatures.

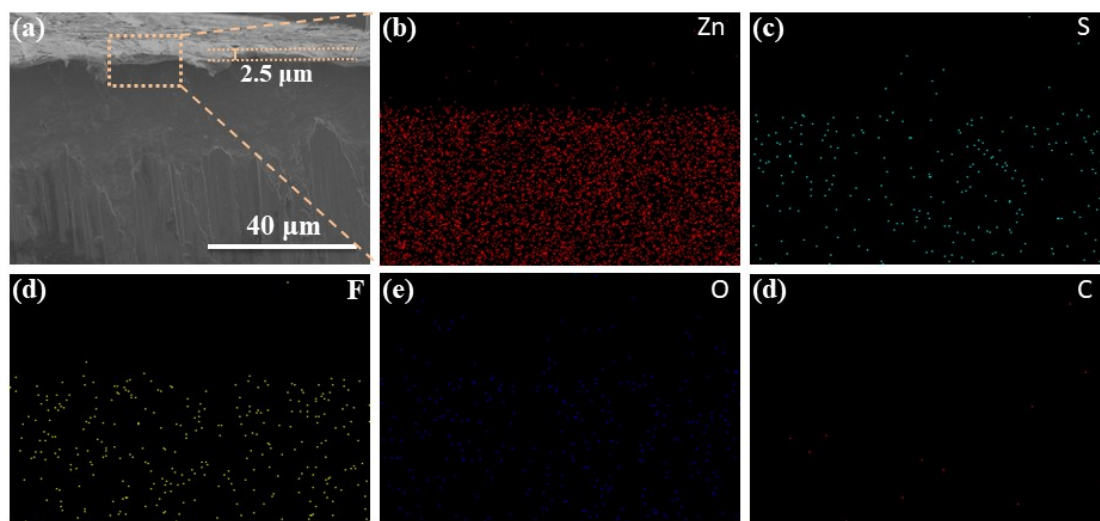


Figure S25 SEM and mapping images of the cycled Zn anode in TFA electrolyte.

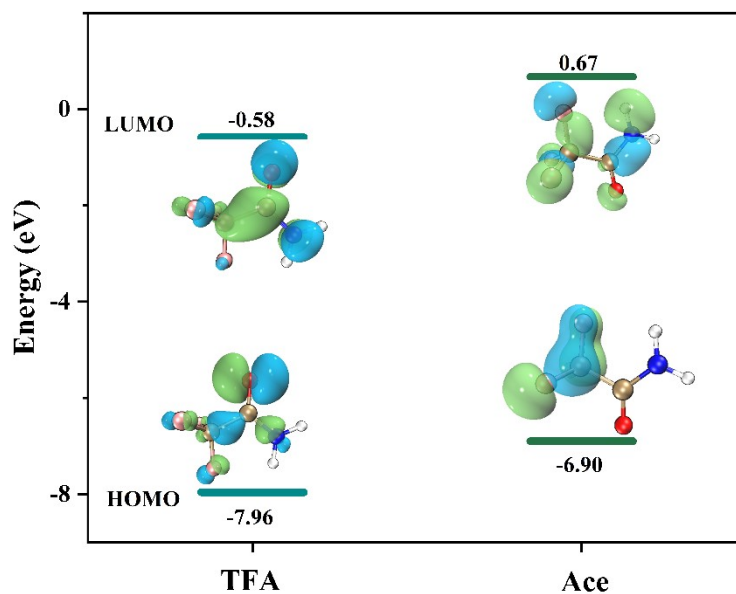


Figure S26 LUMO and HOMO energies of TFA molecules (left) and Ace molecules (right).

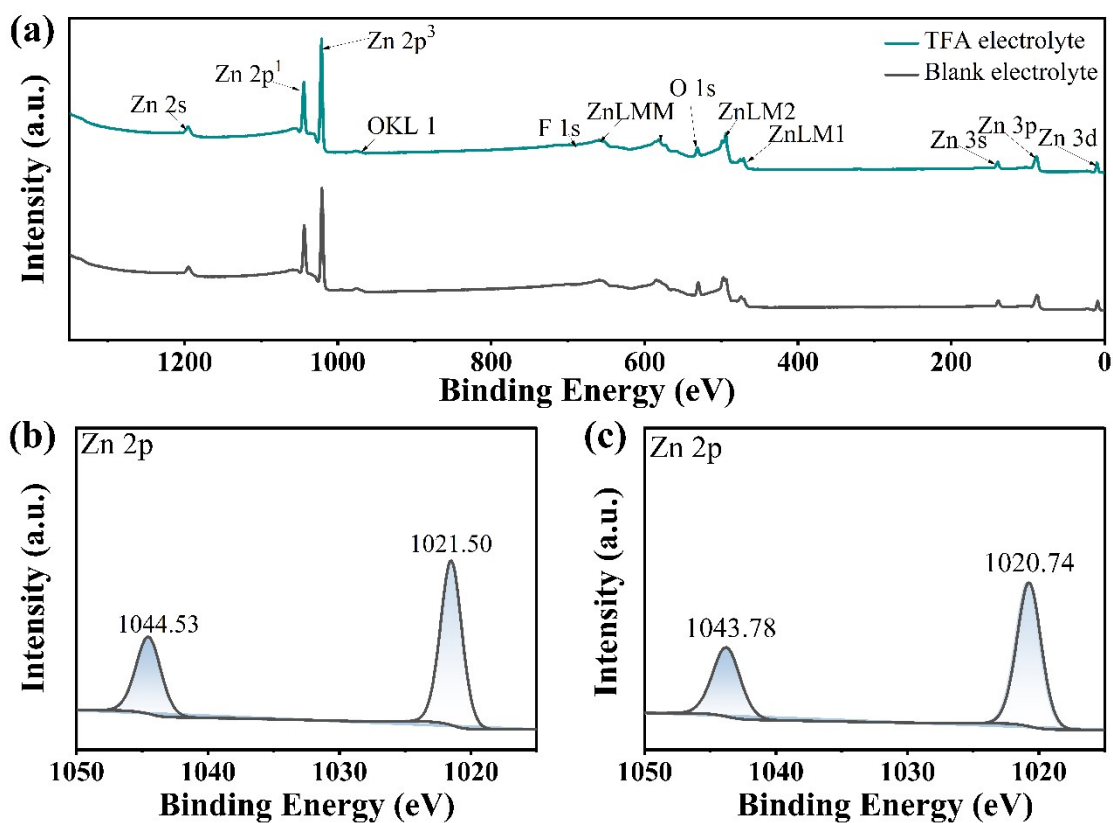


Figure S27 The XPS of Zn anodes cycled in Zn//Zn symmetric cells in TFA and blank electrolytes. (a) XPS full spectrum. (b) Zn 2p of TFA electrolyte. (c) Zn 2p of blank electrolyte.

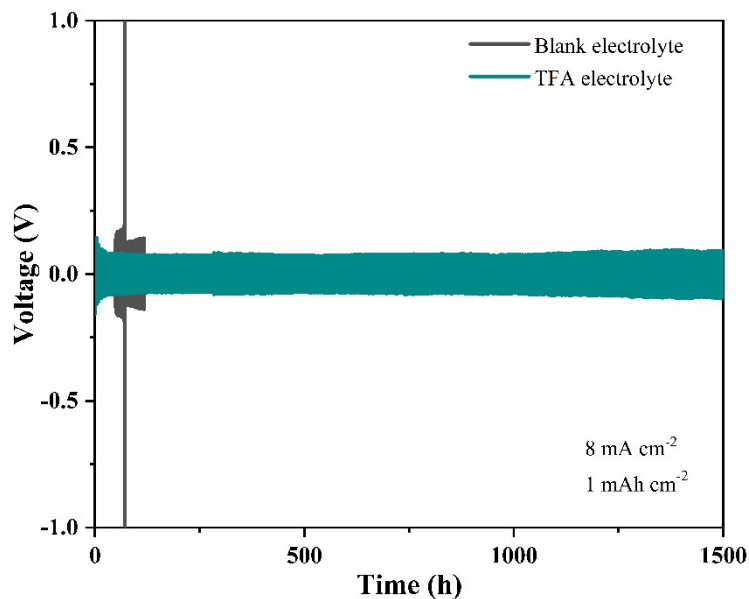


Figure S28 Long-term performance of Zn//Zn symmetrical cells with blank and TFA electrolytes at 8 mA cm^{-2} and 1 mAh cm^{-2} .

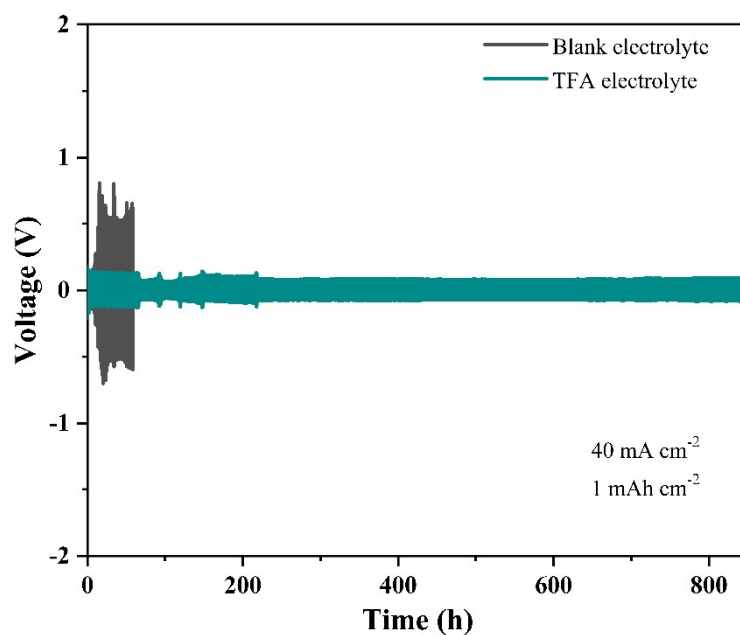


Figure S29 Long-term performance of Zn//Zn symmetrical cells with blank and TFA electrolytes at 40 mA cm^{-2} and 1 mAh cm^{-2} .

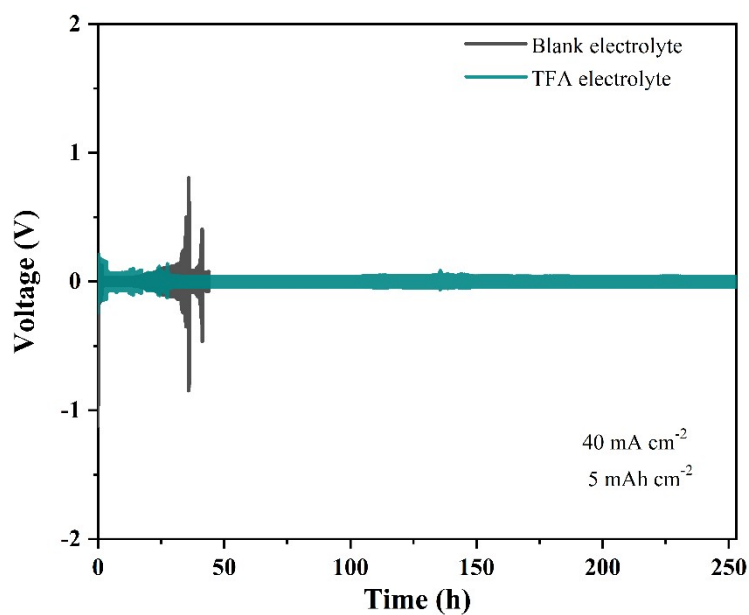


Figure S30 Cycling performance of Zn//Zn symmetrical cells with blank and TFA electrolytes at 40 mA cm^{-2} and 5 mAh cm^{-2} , respectively.

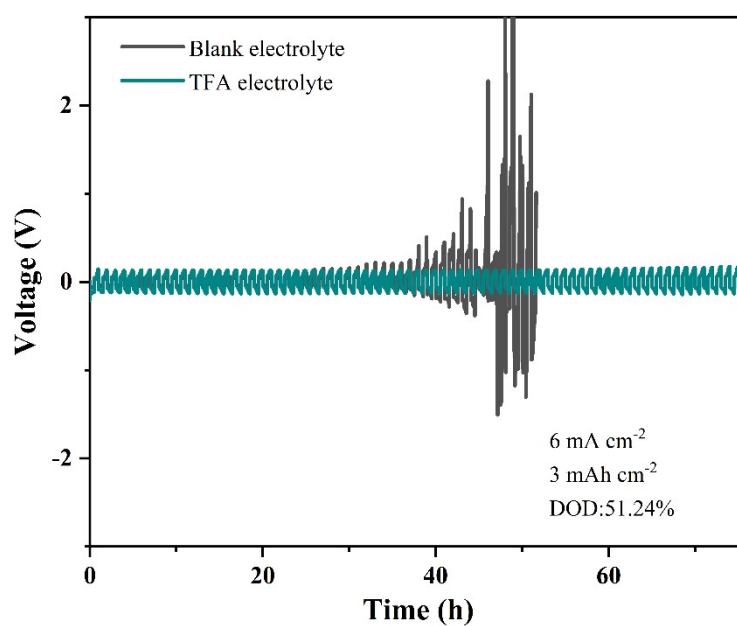


Figure S31 Galvanostatic Zn plating/stripping in Zn//Zn symmetric cells with blank and TFA electrolytes at 6 mA cm^{-2} and 3 mAh cm^{-2} with a high DOD of 51.24%.

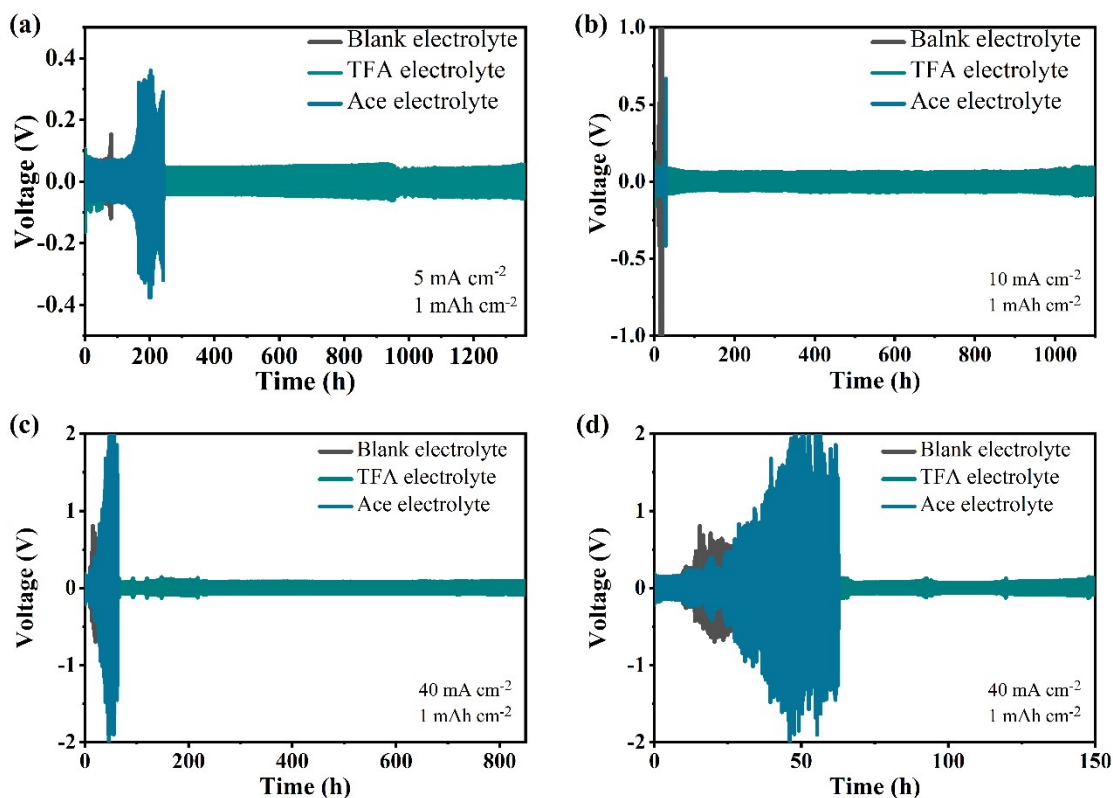


Figure S32 Long-term cycling performance of Zn//Zn symmetrical cells with blank, TFA and Ace electrolytes at various current densities and capacities at (a) 5 mA cm^{-2} , 1 mAh cm^{-2} ; (b) 10 mA cm^{-2} , 1 mAh cm^{-2} ; (c) 40 mA cm^{-2} , 1 mAh cm^{-2} , and (d) 40 mA cm^{-2} , 1 mAh cm^{-2} .

As shown in Figure S30, after 134 h of cycling at a current density of 5 mA cm^{-2} , the polarization voltage of the Zn//Zn symmetric cells containing Ace increased dramatically due to the growth of Zn dendrites. It can be demonstrated that Ace electrolyte can increase the cycle life of symmetric cells (80 h), but the improvement is much less than the effect of TFA electrolyte (1360 h). Even at high current densities (10 mA cm^{-2} and 40 mA cm^{-2}), it is also proved that Ace electrolyte provides much less improvement in the cycle life of symmetric cells than that using TFA electrolyte.

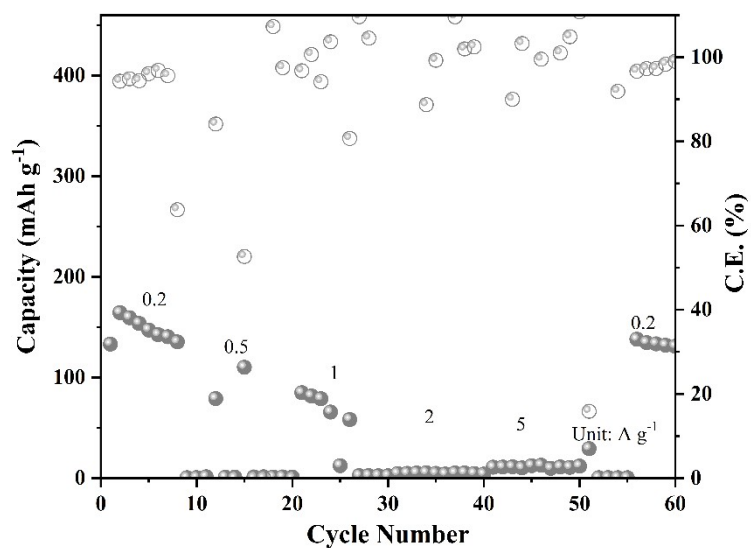


Figure S33 Rate performance of Zn//PT cells at different current densities in blank electrolyte.

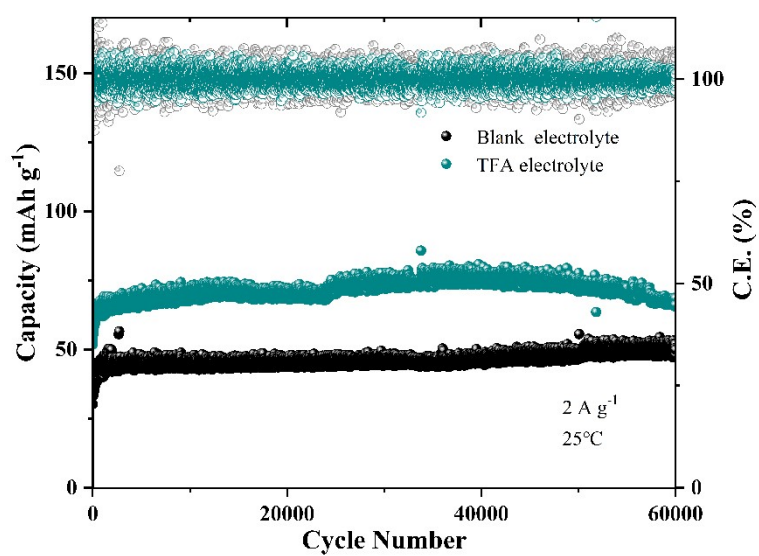


Figure S34 Long-term cycling performance of Zn//AC capacitors with blank and TFA electrolytes at 2 A g^{-1} and in 25°C.

Table S1 EIS of the blank and TFA electrolytes.

		T (°C)	45	55	65	75
Z' (Ω)	Blank electrolyte		0.59	0.48	0.43	0.39
Z' (Ω)	TFA electrolyte		0.58	0.55	0.50	0.46

Table S2 Bond distance of O-H and F-O bonds for different molecule-molecules.

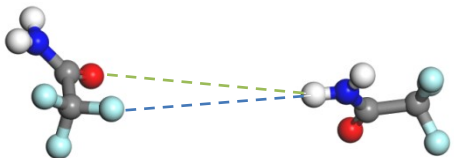
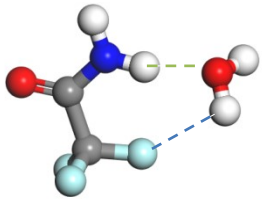
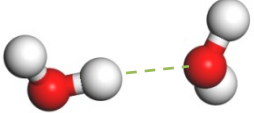
Model	F-H Bond distance (Å)	H-O Bond distance (Å)
	6.40	7.06
	2.76	1.93
	/	1.95

Table S3 Comparison of plating/stripping performance of Zn//Zn symmetric cells.

Ref.	Electrolytes	Plating/stripping time (h)	Current densities (mA cm ⁻²) / Capacity (mAh cm ⁻²)
1	Tetrahydrofuran (THF) additive in ZnSO ₄ electrolyte	600	5/1
2	Polyacrylamide (PAM) additive in ZnSO ₄ electrolyte	110	20/1
3	Threonine (TH) additive in ZnSO ₄ electrolyte	700	5/1
4	propylene glycol (PG) in ZnSO ₄ electrolyte	660	4/2
5	Arginine (Arg) in ZnSO ₄ electrolyte	<100	1.5/0.5
6	Methanol additive in Zn(CF ₃ SO ₃) ₂ electrolyte	100	4/1
7	Ce ³⁺ and La ³⁺ in ZnSO ₄ electrolyte	700	5/1
8	Xylitol in ZnSO ₄ electrolyte	1000	5/1
9	LiCl in ZnSO ₄ electrolyte	170	5/1
10	Ethylene glycol in ZnSO ₄ electrolyte	140	2/1
11	Anion in Zn(CF ₃ SO ₃) ₂ electrolyte	200	10/2
12	Cyclodextrins in ZnSO ₄ electrolyte	160	10/1
13	Hexamethylphosphoramide in Zn(CF ₃ SO ₃) ₂ electrolyte	70	20/4
Our work	Trifluoroacetamide (TFA) in ZnSO₄ electrolyte	1360	5/1
		1100	10/1
		280	40/5

References

1. W. He, Y. Ren, B. S. Lamsal, J. Pokharel, K. Zhang, P. Kharel, J. J. Wu, X. Xian, Y. Cao and Y. Zhou, *ACS Appl. Mater. Inter.*, 2023, **15**, 6647-6656.
2. Q. Zhang, J. Luan, L. Fu, S. Wu, Y. Tang, X. Ji and H. Wang, *Angew. Chem. Int. Ed.*, 2019, **58**, 15841-15847.
3. Z. Miao, Q. Liu, W. Wei, X. Zhao, M. Du, H. Li, F. Zhang, M. Hao, Z. Cui, Y. Sang, X. Wang, H. Liu and S. Wang, *Nano Energy*, 2022, **97**, 107145-107155.
4. Y. Shang, P. Kumar, T. Musso, U. Mittal, Q. Du, X. Liang and D. Kundu, *Adv. Funct. Mater.*, 2022, **32**, 2200606-2200616.
5. Z. Chen, H. Chen, Y. Che, L. Cheng, H. Zhang, J. Chen, F. Xie, N. Wang, Y. Jin and H. Meng, *ACS Sustainable Chem. Eng.*, 2021, **9**, 6855-6863.
6. X. S. Lin, Z. R. Wang, L. H. Ge, J. W. Xu, W. Q. Ma, M. M. Ren, W. L. Liu, J. S. Yao and C. B. Zhang, *ChemElectroChem*, 2022, **9**, e202101724.
7. Y. Li, P. Wu, W. Zhong, C. Xie, Y. Xie, Q. Zhang, D. Sun, Y. Tang and H. Wang, *Energy Environ. Sci.*, 2021, **14**, 5563-5571.
8. H. Wang, W. Ye, B. Yin, K. Wang, M. S. Riaz, B.-B. Xie, Y. Zhong and Y. Hu, *Angew. Chem. Int. Ed.*, 2023, **62**, e202218872.
9. X. Guo, Z. Zhang, J. W. Li, N. J. Luo, G. L. Chai, T. S. Miller, F. L. Lai, P. Shearing, D. J. L. Brett, D. L. Han, Z. Weng, G. J. He and I. P. Parkin, *ACS Energy Lett.*, 2021, **6**, 395-403.
10. N. Chang, T. Li, R. Li, S. Wang, Y. Yin, H. Zhang and X. Li, *Energy Environ. Sci.*, 2020, **13**, 3527-3535.
11. D. Yuan, J. Zhao, H. Ren, Y. Chen, R. Chua, E. T. J. Jie, Y. Cai, E. Edison, W. Manalastas, M. W. Wong and M. Srinivasan, *Angew. Chem. Int. Ed.*, 2021, **60**, 7213-7219.
12. K. Zhao, G. Fan, J. Liu, F. Liu, J. Li, X. Zhou, Y. Ni, M. Yu, Y.-M. Zhang, H. Su, Q. Liu and F. Cheng, *J. Am. Chem. Soc.*, 2022, **144**, 11129-11137.
13. M. Kim, J. Lee, Y. Kim, Y. Park, H. Kim and J. W. Choi, *J. Am. Chem. Soc.*, 2023, **145**, 15776-15787.